

Table III. Infrared Spectra^a of Osmium-salen Complexes in the 1650-1500-cm⁻¹ Region

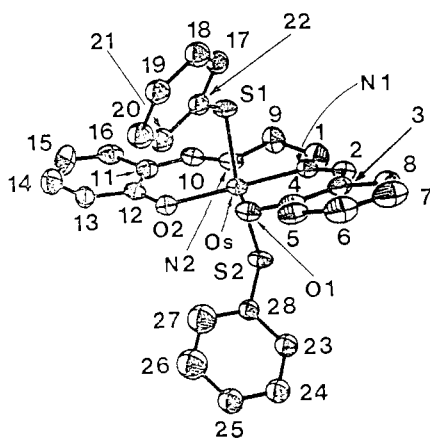
complexes	absorption bands, cm ⁻¹
1	1630 (s), 1595 (s), 1525 (m)
2a	1605 (s), 1590 (s), 1530 (s)
2b	1600 (s), 1590 (s), 1530 (s)
3	1600 (s), 1525 (s)

^aAll spectra were measured as Nujol mulls on KBr or NaCl plates. Abbreviations: s, strong; m, medium.

Table IV. ¹H NMR Spectral Data^a for Os(IV)-salen Complexes

complexes	aromatic protons	azomethine protons	ethylene bridge protons	axial ligand protons
2a	6.60-8.10 (m)	6.24 (s)	2.86	8.95 (s)
2b	6.55-8.06 (m)	6.18 (s)	2.90 (s)	9.8 (t), -0.13 (q)
3	5.78-8.26 (m)	12.0 (s)	2.80 (s)	b

^aNMR spectra were recorded in CD₂Cl₂ solutions, and chemical shift (δ) values were reported from Me₄Si ($\delta = 0.0$) as internal standard. The patterns of the signals were given in parentheses. Abbreviations: s, singlet; q, quartet; t, triplet; m, multiplet. ^bObscured by aromatic protons of the chelate.

**Figure 3.** Persepective view of 3. Thermal ellipsoids are drawn at the 30% probability level.

where H₄-CHBA-Et stands for 1,2-bis(3,5-dichloro-2-hydroxybenzamido)ethene. The Os-S(1) and Os-S(2) bonds measure 2.298 (2) and 2.343 (2) Å, respectively, which are appreciably shorter than the Os(IV)-S bond distances (2.36-2.45 Å) in [Os₂(Et₂dtc)₂][PF₆]₂ (Et₂dtc = N,N'-diethyldithiocarbamate).¹⁰ The Os-N bond distances (Os-N(1) = 2.000 (8) Å and Os-N(2) = 1.993 (7) Å) are normal, and bond lengths and angles for the salen ligand are in agreement with the mean values reported for a series of salen complexes.¹¹

Acknowledgment. This research was supported by the Committee of Conference and Research Grants of the University of Hong Kong (C.-M.C and W.-K.C.). W.-K.C. acknowledges a graduate studentship from the Croucher Foundation.

Registry No. 1, 99727-74-9; 2a, 99748-39-7; 2b, 99727-75-0; 3, 99727-76-1; K₂[OsO₂(OH)₄], 77347-87-6.

Supplementary Material Available: Tables of anisotropic temperature factors, atomic coordinates and thermal parameters of hydrogen atoms, and structure factors (25 pages). Ordering information is given on any current masthead page.

(9) See for example: Anson, F. C.; Christie, J. A.; Collins, T. J.; Coots, R. J.; Furutani, T. T.; Gipson, S. J.; Keech, J. T.; Kraft, T. E.; Santarsiero, B. D.; Spies, G. H. *J. Am. Chem. Soc.* **1984**, *106*, 4460.

(10) Wheeler, S. H.; Pignolet, L. H. *Inorg. Chem.* **1980**, *19*, 972.

(11) Calligaris, M.; Nardin, G.; Randascio, L. *Coord. Chem. Rev.* **1972**, *7*, 385.

Contribution from the Department of Chemistry, Columbia University in the City of New York, New York, New York 10027

Effects of Optical Density, Extinction Coefficient, and Window Area on Quantum Yields: Application to Mechanistic Problems in Organometallic Photochemistry

Alan S. Goldman and David R. Tyler*

Received March 7, 1985

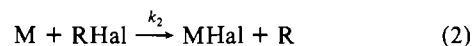
We and others¹⁻³ have investigated the effects of light intensity on observed quantum yields. To the best of our knowledge, however, it has not been pointed out in the literature that parameters such as the extinction coefficient and window area can also have pronounced effects on the observed quantum yield. In particular, because the quantum yield can vary with the extinction coefficient, a change in the observed quantum yield corresponding to a change in wavelength may be due only to the different extinction coefficients at the respective wavelengths. In such a case, any conclusions regarding the photochemistry or photophysics drawn on the assumption of a true wavelength effect will be incorrect. In this note we quantify the effects that optical density, radiation intensity, and window area can have on the observed quantum yield, and we discuss the origin of these effects.

Results and Discussion

Although it is relatively simple to distribute heat homogeneously throughout a reaction solution, it is rare that a photoreaction solution will be "homogeneous in photons". As a result of both the Beer-Lambert law and the fact that radiation is typically not focused evenly over the entire surface of the reaction vessel, each point within the reaction mixture will experience a different photon flux. For an intramolecular reaction (e.g. olefin cis-trans isomerization) this phenomenon will not affect the quantum yield. However, when a reaction that is first order in a short-lived intermediate is in competition with a second-order reaction between two photoproduct species, the quantum yield will be affected by the local steady-state concentrations of these transient photoproducts and, therefore, by the amount of light absorbed at each point in the solution. The extent to which stirring can homogenize the solution depends upon the lifetimes of these species; it must be remembered that stirring can be slow on the time scale of many "fast" intermolecular reactions.

Reactions involving radicals are probably the most common type of reaction in which the quantum yield can be affected by the local steady-state concentrations of transient intermediates. As an example, consider the radical reaction in Scheme I in which a photogenerated metal radical abstracts a halogen atom from an alkyl halide.

Scheme I



M-M = a metal-metal-bonded dimer, e.g. Mn₂(CO)₁₀;

RHal = an alkyl halide; M = a metal radical, e.g. Mn(CO)₅

As we show in the Appendix, the overall quantum yield for disappearance of the dimer is given by

$$\phi_t = \frac{2b\phi_p}{(1-T)} \left[\frac{-(\ln 10)b\epsilon CL}{z} + \frac{2}{z}(b^2 - zT)^{1/2} - \frac{2}{z}(b^2 - z)^{1/2} + \frac{b}{z} \ln \left(\frac{(b^2 - zT)^{1/2} - b}{(b^2 - zT)^{1/2} + b} \right) - \frac{b}{z} \ln \left(\frac{(b^2 - z)^{1/2} - b}{(b^2 - z)^{1/2} + b} \right) \right] \quad (3)$$

where T = transmittance of the solution ($10^{-\epsilon CL}$), ϵ = extinction

* To whom correspondence should be addressed at the Department of Chemistry, University of Oregon, Eugene, OR 97403.

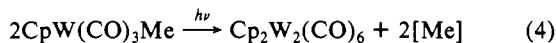
Table I. Quantum Yields for Scheme I Calculated by Using Eq 3 ($\phi_p = 0.4$, $L = 1.0$ cm)

Conditions: $I_0 = 10^{-8}$ einstein/s, $k_{-1} = 10^9$ M $^{-1}$ s $^{-1}$, $k_2[\text{RHal}] = 100$ s $^{-1}$, $A = 3$ cm 2 , $C = 0.005$ M			
ϵ/M^{-1} cm $^{-1}$	ϕ	ϵ/M^{-1} cm $^{-1}$	ϕ
10	0.379	10000	0.082
100	0.308	40000	0.045
1000	0.192		
Conditions: $I_0 = 10^{-8}$ einstein/s, $k_{-1} = 10^9$ M $^{-1}$ s $^{-1}$, $k_2[\text{RHal}] = 100$ s $^{-1}$, $\epsilon = 100$ M $^{-1}$ cm $^{-1}$, $C = 0.005$ M			
A/cm^2	ϕ	A/cm^2	ϕ
30	0.385	0.03	0.060
3	0.308	0.0075	0.031
0.3	0.159		
Conditions: $I_0 = 10^{-8}$ einstein/s, $k_{-1} = 10^9$ M $^{-1}$ s $^{-1}$, $k_2[\text{RHal}] = 100$ s $^{-1}$, $A = 3$ cm 2 , $\epsilon = 1000$ M $^{-1}$ cm $^{-1}$			
$C/10^{-3}$ M	ϕ	$C/10^{-3}$ M	ϕ
200	0.045	0.5	0.308
50	0.082	0.05	0.379
5	0.192		
Conditions: $k_{-1} = 10^9$ M $^{-1}$ s $^{-1}$, $k_2[\text{RHal}] = 100$ s $^{-1}$, $A = 3$ cm 2 , $C = 0.005$ M, $\epsilon = 1000$ M $^{-1}$ cm $^{-1}$			
$I_0/(\text{einstein/s})$	ϕ	$I_0/(\text{einstein/s})$	ϕ
1×10^{-9}	0.327	1×10^{-6}	0.030
1×10^{-8}	0.192	4×10^{-6}	0.015
1×10^{-7}	0.082		
Conditions: $I_0 = 10^{-8}$ einstein/s, $k_2[\text{RHal}] = 100$ s $^{-1}$, $A = 3$ cm 2 , $C = 0.005$ M, $\epsilon = 1000$ M $^{-1}$ cm $^{-1}$			
k_{-1}/M^{-1} s $^{-1}$	ϕ	k_{-1}/M^{-1} s $^{-1}$	ϕ
1×10^7	0.388	1×10^{10}	0.082
1×10^8	0.326	4×10^{10}	0.045
1×10^9	0.192		
Conditions: $I_0 = 10^{-8}$ einstein/s, $k_{-1} = 10^9$ M $^{-1}$ s $^{-1}$, $A = 3$ cm 2 , $C = 0.005$ M, $\epsilon = 1000$ M $^{-1}$ cm $^{-1}$			
$k_2[\text{RHal}]/\text{s}^{-1}$	ϕ	$k_2[\text{RHal}]/\text{s}^{-1}$	ϕ
1000	0.389	1.0	0.0032
100	0.192	0.1	3.2×10^{-4}
10	0.030		

coefficient of M-M at the wavelength of irradiation, $L =$ cell pathlength, $C =$ concentration of M-M, $\phi_p =$ quantum yield of primary photoprocess (metal-metal bond homolysis), $b = -k_2/[\text{RHal}]$, $z = -16k_{-1}\phi_p I_0 C (\ln 10)/(A/1000)$, $I_0 =$ incident radiation intensity, and $A =$ area of surface irradiated by incident radiation.

Table I shows numerically how ϵ , C , I_0 , and A can affect the observed quantum yield. Note that ϕ_t as a function of optical density, I_0 , or $1/A$ follows the same pattern. In the limit of low values of these parameters ϕ_t is nearly equal to ϕ_p , and in the limit of high values (low values of ϕ_t/ϕ_p) ϕ_t is inversely proportional to the square root of the parameter. Thus, if these parameters are not accounted for, quantum yield data for radical reactions proceeding according to Scheme I or a related pathway should be viewed with skepticism, unless the experimenter can be sure that the reactions were run under "limiting case" conditions.

We found another type of reaction, not completely analogous to that of Scheme I, in which the quantum yield is dependent on the parameters discussed above, namely, the binuclear elimination reaction of $\text{CpW}(\text{CO})_3\text{Me}$ ($\text{Me} = \text{CH}_3$; $\text{Cp} = \eta^5\text{-C}_5\text{H}_5$):



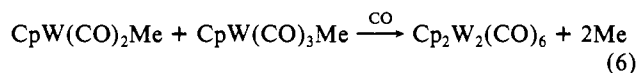
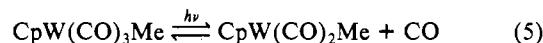
- (1) (a) Yang, N. C.; Murov, S. *J. Am. Chem. Soc.* **1966**, *88*, 2852-2854. (b) Schuster, D. I.; Barile, G. C.; Liu, K. *J. Am. Chem. Soc.* **1975**, *97*, 4441-4443. (c) Rubin, M. B.; Inbar, S. *J. Am. Chem. Soc.* **1978**, *100*, 2266-2268.
(2) Fox, A.; Poë, A. *J. Am. Chem. Soc.* **1980**, *102*, 2497-2499.
(3) Tyler, D. R. *J. Photochem.* **1982**, *20*, 101-106.

Table II. Quantum Yields for Reaction 9^a

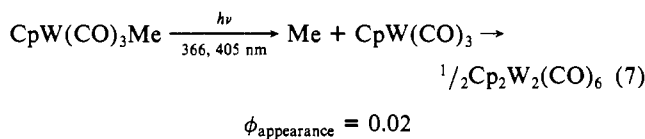
λ/nm (ϵ/M^{-1} cm $^{-1}$)	$I_0/(\text{einstein/s})$	$\phi_{\text{obsd}} - 0.02^b$	ϕ_{calcd}^c
366 (900)	1.7×10^{-7}	0.086	0.090
366 (900)	1.7×10^{-6}	0.042	0.033
405 (200)	9.2×10^{-7}	0.083	(0.083)

^aIn benzene. Solution volume equals 3 mL; $L = 1.0$ cm. ^b0.02 subtracted to correct for reaction 7. ^c $k_2/k_{-1}^{1/2}$ set equal to 8.7×10^{-3} M $^{1/2}$ s $^{-1/2}$.

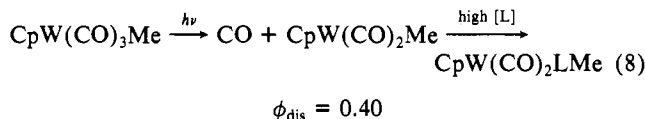
This reaction is probably somewhat of a rarity among reactions in which irradiation parameters affect quantum yields in that it does not involve radicals. Rather, the dominant primary photoprocess is metal-carbonyl bond dissociation;⁴ we have suggested the mechanism



We found that dimerization under argon proceeds with a quantum yield (for dimer appearance) of 0.103 at 405 nm with an intensity of 9.15×10^{-7} einstein/min. At 366 nm, with an intensity of 1.7×10^{-6} einstein/min, the quantum yield is 0.062, whereas with an intensity of 1.7×10^{-7} the quantum yield is 0.106. Thus, the overall quantum yield is a function of both wavelength and intensity. (A value of 0.02 should be subtracted from all three quantum yields to obtain the quantum yield for dimerization via eq 5 and 6; this correction is necessary because dimerization due to tungsten-methyl bond cleavage (eq 7) also occurs,⁵ inde-



pendently of reactions 5 and 6.) However, because the limiting substitution (eq 8) quantum yield, ϕ_{dis} , for the complex is the same



at 366 and 405 nm (0.40) and independent of intensity, we can safely conclude that the dimerization quantum yields do not reflect different primary photoprocess quantum yields; i.e., we are not observing a "true" wavelength effect. The variations in the quantum yield result from changes in the intensity and extinction coefficient which affect the local steady-state concentration of the intermediate and free CO (which in turn affect the rate of the back-reaction of eq 5). It should be noted that the kinetics of reactions 5 and 6 can essentially be described by eq 3. The overall quantum yield of the reaction is

$$\phi = \phi_{\text{dis}}(k_2[\text{CpW}(\text{CO})_3\text{Me}]) / (k_{-1}[\text{CO}] + k_2[\text{CpW}(\text{CO})_3\text{Me}]) \quad (9)$$

If the assumption is made that the steady-state concentration of CO is equal to that of the fragment, $\text{CpW}(\text{CO})_2\text{Me}$,⁶ then eq 9 takes the same form as eq 10 in the Appendix and eq 3 is applicable with $b = -k_2[\text{CpW}(\text{CO})_3\text{Me}]$. (Note that the low

- (4) (a) Severson, R. G.; Wojcicki, A. *J. Organomet. Chem.* **1978**, *157*, 173-185. (b) Tyler, D. R. *Inorg. Chem.* **1981**, *20*, 2257, 2261.
(5) Goldman, A. S.; Tyler, D. R. *J. Am. Chem. Soc.* **1986**, *108*, 89-94.
(6) More rigorously, the steady-state concentration of CO should be set equal to the combined steady-state concentrations of $\text{CpW}(\text{CO})_2\text{Me}$ and $\text{Cp}_2\text{W}_2(\text{CO})_6$; thus the assumption is only valid to the extent that $[\text{CpW}(\text{CO})_2\text{Me}] \gg [\text{Cp}_2\text{W}_2(\text{CO})_6]$. However, as long as $[\text{CO}]$ is greater than $[\text{CpW}(\text{CO})_2\text{Me}]$ by a relatively constant factor, then the form of the equation is unchanged.

steady-state concentration of CO is unusual for reactions resulting from metal-carbonyl bond dissociation (e.g. ligand substitution) because there is usually a stoichiometric increase in [CO] in such reactions.) As a result of the low concentration of CO in the solution of reaction 4, coordination of the very poor ligand, CpW(CO)₃Me (eq 6) is competitive with the back-reaction of CpW(CO)₂Me with CO (eq 5).

Table II shows a comparison of the observed values of ϕ compared with those calculated from eq 3. The value of ϕ_p was assumed to be 0.40, the quantum yield for ligand substitution. The rate constants k_{-1} and k_2 were set so as to let ϕ_{calcd} equal ϕ_{obsd} for the case in which wavelength is equal to 405 nm. It can be seen that the quantum yield is in fact lowered by increasing the extinction coefficient and intensity, although not to as great an extent as predicted. Several factors could substantially detract from the agreement between predicted and observed values in the use of eq 3: (1) the inability to reproducibly focus the lamp on the reaction cell will result in an effective variability of A ; (2) stirring may occur on a time scale competitive with the lifetimes of the intermediates (this will decrease the effect of A and ϵ on the observed values); (3) in the particular case of reactions 5 and 6, a buildup of CO in solution, perhaps due to a side reaction, would result in an overall rate of back-reaction less dependent on intensity, A , and ϵ .

Conclusion. Certain photochemical pathways involve a competition between elementary reactions that are first and second order in a short-lived intermediate. The observed quantum yields of such reactions may show a dependency on irradiation parameters such as optical density, extinction coefficient, irradiation intensity, and window area. Difficulties may be encountered in attempting to quantitatively apply the above equations with any precision. Nevertheless, we believe that they can be quite useful, if only for calculating the expected direction and order of magnitude of any dependency of the quantum yield on these irradiation parameters. At the very least, the photochemical experimenter should always be aware of the possibility that the parameters discussed herein can affect efficiencies and even product distributions.

Experimental Section

Quantum yield measurements for the binuclear reductive elimination of CpW(CO)₃Me (0.02 M in benzene) were made by monitoring the band maximum at 508 nm of the product complex Cp₂W₂(CO)₆ with a Beckman DU spectrophotometer. The light source for irradiations was a 200-W Oriel high-pressure mercury lamp. Intensities were varied with use of Oriel neutral-density filters. Each value was based on three independent sets of three consecutive irradiations. Substitution quantum yields were determined by monitoring the 2016- and 1918-cm⁻¹ bands of CpW(CO)₃Me and the 1933- and 1847-cm⁻¹ bands of CpW(CO)₂(PPh₃)Me with a Perkin-Elmer 983 spectrophotometer. Lamp intensities were measured by ferrioxalate actinometry. The 366- and 405-nm mercury arc bands were isolated with use of a Corning CS 7-83 filter and an Edmund Scientific interference filter, respectively. CpW(CO)₃Me was prepared by literature methods.⁷ All other materials were obtained commercially. Benzene was distilled under nitrogen from LiAlH₄.

Acknowledgment. This research was supported by the National Science Foundation. We thank Steven L. Peterson for technical assistance and Sam B. Collins and Professor Bill Troglor for helpful discussions.

Appendix

The observed quantum yield for the reaction in Scheme I will be dependent on the competition between the forward reaction and the back-reaction, the latter of which is dependent on the steady-state concentration of M. The quantum yield at any given point X in solution will be

$$\phi_X = \phi_p k_2 [\text{RHal}] / (2k_{-1} [\text{M}]_X + k_2 [\text{RHal}]) \quad (10)$$

where ϕ_p is the quantum yield for the primary photoprocess (metal-metal bond homolysis) and $[\text{M}]_X$ is the steady state concentration of [M] at point X. Let us assume a rectangular-

prism reaction cell of pathlength L , evenly irradiated over all or part of one surface, with the incident light, perpendicular to the irradiated surface, distributed over area A . Let x equal the distance of point X from the irradiated surface, ϵ equal the extinction coefficient of M-M at the wavelength of irradiation, I_0 equal the incident radiation intensity, and C equal the concentration of M-M. Using the steady-state approximation for M, we then find

$$[\text{M}]_X = \frac{b + (b^2 + 8k_{-1}f)^{1/2}}{4k_{-1}} \quad (11)$$

where

$$b = -k_2 [\text{RHal}] \quad (12)$$

$$f = (2\phi_p I_0 \epsilon C (\ln 10) 10^{-\epsilon C x}) / (A/1000) \quad (13)$$

The value for the overall quantum yield ϕ_t can be obtained by integration over the length of the cell (from $x = 0$ to L):

$$\phi_t = \frac{(\ln 10) \epsilon C}{(1 - T)} \int_{x=0}^{x=L} \frac{\phi_x I_x}{I_0} dx \quad (14)$$

where $I_x = I_0 10^{-\epsilon C x}$ is the intensity at point x . Making the substitution $u = 10^{-\epsilon C x}$ and integrating, we find

$$\phi_t = \frac{2b\phi_p}{(1 - T)} \left[\frac{-(\ln 10)b\epsilon CL}{z} + \frac{2}{z} (b^2 - zT)^{1/2} - \frac{2}{z} (b^2 - z)^{1/2} + \frac{b}{z} \ln \left(\frac{(b^2 - zT)^{1/2} - b}{(b^2 - zT)^{1/2} + b} \right) - \frac{b}{z} \ln \left(\frac{(b^2 - z)^{1/2} - b}{(b^2 - z)^{1/2} + b} \right) \right] \quad (3)$$

where T is the transmittance of the solution ($10^{-\epsilon CL}$) and $z = -16k_{-1}\phi_p I_0 \epsilon C (\ln 10) / (A/1000)$.

Registry No. Mn₂(CO)₁₀, 10170-69-1; Mn(CO)₅, 14971-26-7; CpW(CO)₃Me, 12082-27-8; Cp₂W₂(CO)₆, 12091-65-5; CpW(CO)₂(PPh₃)Me, 12115-41-2.

Contribution from the Department of Chemistry, Faculty of Science, Tohoku University, Sendai 980, Japan

Kinetics of the Ligand Substitution Reactions of a Labilized Chromium(III) Complex, [(NH₃)₅Co(edta)Cr(H₂O)]²⁺

Hiroshi Ogino,* Akihiko Masuko, Setsuo Ito, Naoko Miura, and Makoto Shimura

Received July 24, 1985

The EDTA and related polyamino polycarboxylate ligands have been shown to labilize greatly the ligand substitution reactions of the chromium(III) complexes.¹ Later, trivalent metal complexes other than those of chromium(III), including titanium(III), iron(III), cobalt(III), ruthenium(III), and osmium(III) complexes, were also found to undergo rapid ligand substitution reactions when an EDTA-type ligand was coordinated.²⁻⁶ This remarkable effect of the EDTA-type ligand has attracted continuing attention for a decade.⁷

- (1) Ogino, H.; Watanabe, T.; Tanaka, N. *Inorg. Chem.* 1975, 14, 2093.
- (2) Lee, R. A.; Earley, J. E. *Inorg. Chem.* 1981, 20, 1739.
- (3) Thompson, G. A. K.; Sykes, A. G. *Inorg. Chem.* 1979, 18, 2025.
- (4) Ogino, H.; Shimura, M.; Tanaka, N. *Inorg. Chem.* 1979, 18, 2497.
- (5) Matsubara, T.; Creutz, C. *Inorg. Chem.* 1979, 18, 1956.
- (6) Ogino, H.; Shimura, M. *Adv. Inorg. Bioinorg. Mech.* 1985, 4.
- (7) Abbreviations used in this note: EDTA, ethylenediamine-*N,N,N',N'*-tetraacetate; HEDTRA, *N*-(hydroxyethyl)ethylenediamine-*N,N',N'*-triacetate; OAc⁻, acetate.

(7) See ref 4b, Experimental Section, and references therein.